Electrochimica Acta 546 (2026) 147790

Contents lists available at ScienceDirect

Electrochimica Acta

journal homepage: www.journals.elsevier.com/electrochimica-acta

Applicability range of potential step chronoamperometry for determining reliable diffusion coefficients of hydrogen and lithium in host materials

Magdalena Seiler *, Giorgia Guardi, Stefan Wagner, Astrid Pundt

ARTICLE INFO

Dataset link: Data from "Applicability range of Potential Step Chronoamperometry for the Determination of the Diffusion Coefficients of Hydrogen and Lithium in Host Materials" (Original data)

Keywords:
Potential step chronoamperometry
Potentiostatic current transient
Diffusion coefficient
Electrochemical loading
Hydrogen

ABSTRACT

Potential step chronoamperometry is often used to study the electrochemical unloading process and to determine the diffusion coefficient D of an intercalating atom species in a host material, as it is seemingly easily applicable. The present work emphasises the importance of ensuring a diffusion-controlled unloading process during the potential step chronoamperometry measurement, if determination of the diffusion coefficient is targeted. As an example, diffusion-controlled and non-diffusion-controlled hydrogen unloading series from palladium samples and the resulting diffusion coefficients are presented, for comparison. A literature review summarising the diffusion coefficients of different intercalating species determined for several different systems by this method reveals a systematic error in the results. It turned out that insufficient diffusion control is a common issue in the application of the chronoamperometry method. Based on this finding, it is suggested to verify measurements in the diffusion-controlled regime when chronoamperometry is applied. A suitable verification technique is provided.

1. Introduction

The diffusion of intercalating species in host materials is scientifically and technologically important in different fields of applications. For example, the diffusion of Li-ions in host materials is studied for battery materials [1], that of hydrogen is studied in the context of hydrogen storage applications [2] and hydrogen embrittlement [3]. The diffusion of these intercalating species is described by the diffusion coefficient $D_{H/Li}$. A relatively simple method for measuring the diffusion coefficient commonly mentioned is potential step chronoamperometry. In this method, the sample is electrochemically loaded with the intercalating species. The potential is then varied in a single step to the discharge potential, releasing the intercalating species from the sample. Investigating the unloading process is preferred in comparison to the loading process, as not all hydrogen or lithium is necessarily absorbed in the sample during the loading process.

In the following, we focus on intercalating hydrogen in materials. There, the unloading process can be described by three steps (Fig. 1). First, the absorbed hydrogen atoms interstitially diffuse through the host material towards the interface with the electrolyte. In the next step, the absorbed hydrogen is adsorbed on the samples surface. In the third step, the adsorbed hydrogen takes part in an electron transfer reaction before leaving the sample surface. The reaction differs depending on whether the electrolyte is acidic or alkaline. For an arbitrary metal M in an alkaline environment the reaction is as follows [4]:

$$[MH]_{ads} + OH^- \rightarrow H_2O + M + e^- \quad (1)$$

Crank [5] or Jost [6] describe diffusion in a sphere or a plane sheet at uniform initial concentration c_0 and a constant surface concentration c_s. They give the relative concentration $(c\text{-}c_0)/(c_s\text{-}c_0)$ at any given time t. The geometry is characterised by the diffusion length L. For a sphere, the diffusion length L is equal to the radius of the sphere. For a plane sheet, that is in contact with the electrolyte on one side of the sample only, the diffusion length L is equal to the sample thickness. In the case of a plane sheet, which is in contact with the electrolyte on both sides, the diffusion length is half of the sample thickness. Using Faraday's law [7], the current resulting from diffusion in a plane sheet with the surface area A is given by Equ. (2).

$$I(t) = \frac{\partial \frac{c - c_0}{c_s - c_0}}{\partial t} \cdot (c_s - c_0) \cdot L \cdot A \cdot F = \frac{2FA(c_s - c_0)D}{L} \sum_{n=0}^{\infty} exp\left(- \frac{D(2n+1)^2 \pi^2}{4L^2} \cdot t \right) \quad (2)$$

To discuss Equ. (2) in general, the current and the time are nomalised

* Corresponding author.
E-mail address: magdalena.seiler@kit.edu (M. Seiler).

https://doi.org/10.1016/j.electacta.2025.147790
Received 25 September 2025; Received in revised form 6 November 2025; Accepted 11 November 2025
Available online 12 November 2025

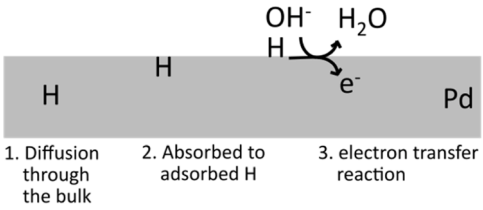

Fig. 1. Schematic drawing of the hydrogen unloading process. The first step is the diffusion of the hydrogen through the Pd. Then, the absorbed hydrogen gets adsorbed on the samples surface. The adsorbed hydrogen takes part in the electron transfer reaction.

according to Equ. (3) and (4) [5].

$$I_{normalised} = \frac{I}{2FA\Delta cD/L} \tag{3}$$

$$t_{normalised} = \frac{tD}{L^2} \tag{4}$$

Fig. 2 shows the calculated current transient due to a potential step in linear representation.

The diffusion coefficient can be obtained from potential step chronoamperometry either by a short-time approximation, using the period of semi-infinite diffusion, or else by a long-time approximation. The short-time approximation has been described for example in the theoretical paper by Montella [8]. This study focuses on the long-time approximation. A concentration independent diffusion coefficient is assumed. To determine the diffusion coefficient using the long-time approximation, only the first term of the sum in Equ. (2) is used. Logarithmising gives the following equation:

$$ln(I) = ln\left(\frac{2FA(c_s - c_0)D}{L}\right) - \frac{\pi^2 D}{4L^2}\cdot t \tag{5}$$

Fig. 3 shows the semi-logarithmic representation of the current transient described by Equ. (2). At longer times, when the current transient is almost linear, it is described by Equ. (5). So when using only the first term in Equ. (2) it is necessary to use the long-time approximation, and the current transient at shorter times cannot be evaluated. To determine the diffusion coefficient, the slope m of the current transient in this period is determined and rearranged (Equ. 6). Equ. 6 is valid for the diffusion in a plane sheet as well as in a sphere [9].

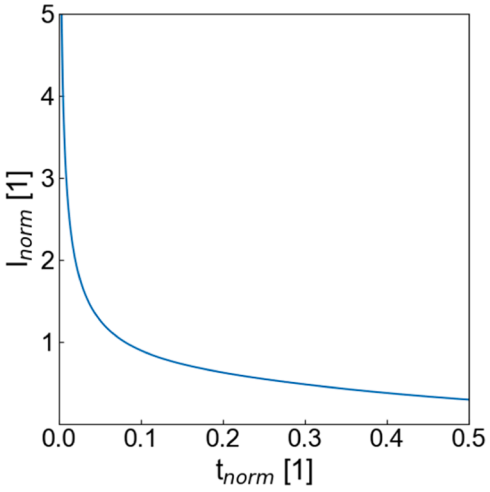

Fig. 2. Calculated current transient of a potential step chronoamperometry measurement of a sheet with thickness L. The current is calculated according to Equ. (2). The current and time axes are normalised according to Equ. (3) and (4). The current transient is shown in a linear representation.

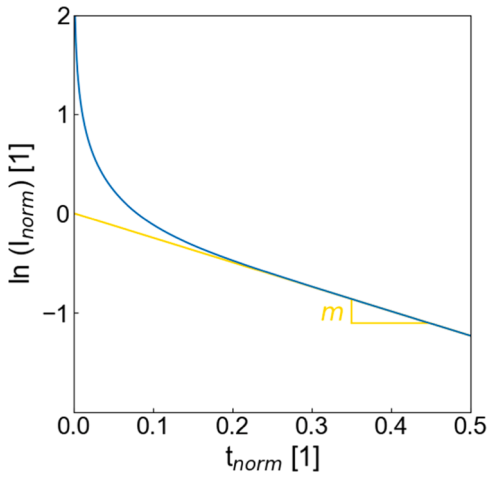

Fig. 3. Calculated current transient of a potential step chronoamperometry measurement of a sheet with thickness L. The current is calculated according to Equ. (2). The current and time axes are normalized according to Equ. (3) and (4). It is a semi-logarithmic representation with a logarithmic current axis. At longer times, the current transient is almost a linear function with slope m.

$$D = \frac{4}{\pi^2}\left|m\right|L^2 \tag{6}$$

Fig. 4(a) shows the normalized and double-logarithmic current transient. It appears linear for shorter times. The derivative shown in Fig. 4(b) is a constant value of $c = -0.5$ during this period. This period is associated with semi-infinite diffusion, during which the finite diffusion length of the sample does not yet have an impact on the current transient [10]. In Fig. 4(c) the derivative of the logarithmic current transient is plotted on a linear time axis. There, the constant value of $c = -0.5$ is followed by a period with a constant slope a. Using the long-time approximation, the derivative of the double-logarithmic representation is calculated by Equ (7).

$$\frac{d\ log(I)}{d\ log(t)} = \frac{d\ log(I)}{dt}\frac{dt}{d\ log(t)} = -\frac{D\pi^2}{4L^2}\cdot t = a\cdot t \tag{7}$$

Rearranging the term for the slope a obtained by Equ. (7) for the diffusion coefficient D yields Equ. (8).

$$D = \frac{4}{\pi^2}\left|a\right|L^2 \tag{8}$$

This representation is described in detail by Montella [8]. The double-logarithmic representation was used earlier by Shin and Pyun [11] to investigate the diffusion of lithium into a $Li_{1-\delta}CoO_2$ electrode.

In 2005, Lee and Pyun reviewed published results using potential step chronoamperometry for determining the diffusion coefficient [10]. They distinguish 1) a process under diffusion-controlled constraint, 2) a process under the constraint of hydrogen transfer from the absorbed state to the adsorbed state and 3) a process under the constraint of interfacial charge transfer. Lee and Pyun demonstrate that the process control does not only depend on the electrode/electrolyte system itself, but also on the applied potential step, the electrolyte resistance and the samples surface. According to Lee and Pyun, for a suitbale determination of the diffusion coefficient the process under investigation has to be in the diffusion-controlled regime. For H in Pd, Lee and Pyun emphasize that the process is scarcely controlled by diffusion. They report a significant impact of traps as well as hydride phase formation on the current transient.

Montella [8] modelled the influence of electron transfer kinetics and ohmic drop effects by numerical calculations of the method. Ohmic drop is the influence of the intrinsic resistance of the electrolyte on the potential [7]. According to Montella, its influence cannot be separated

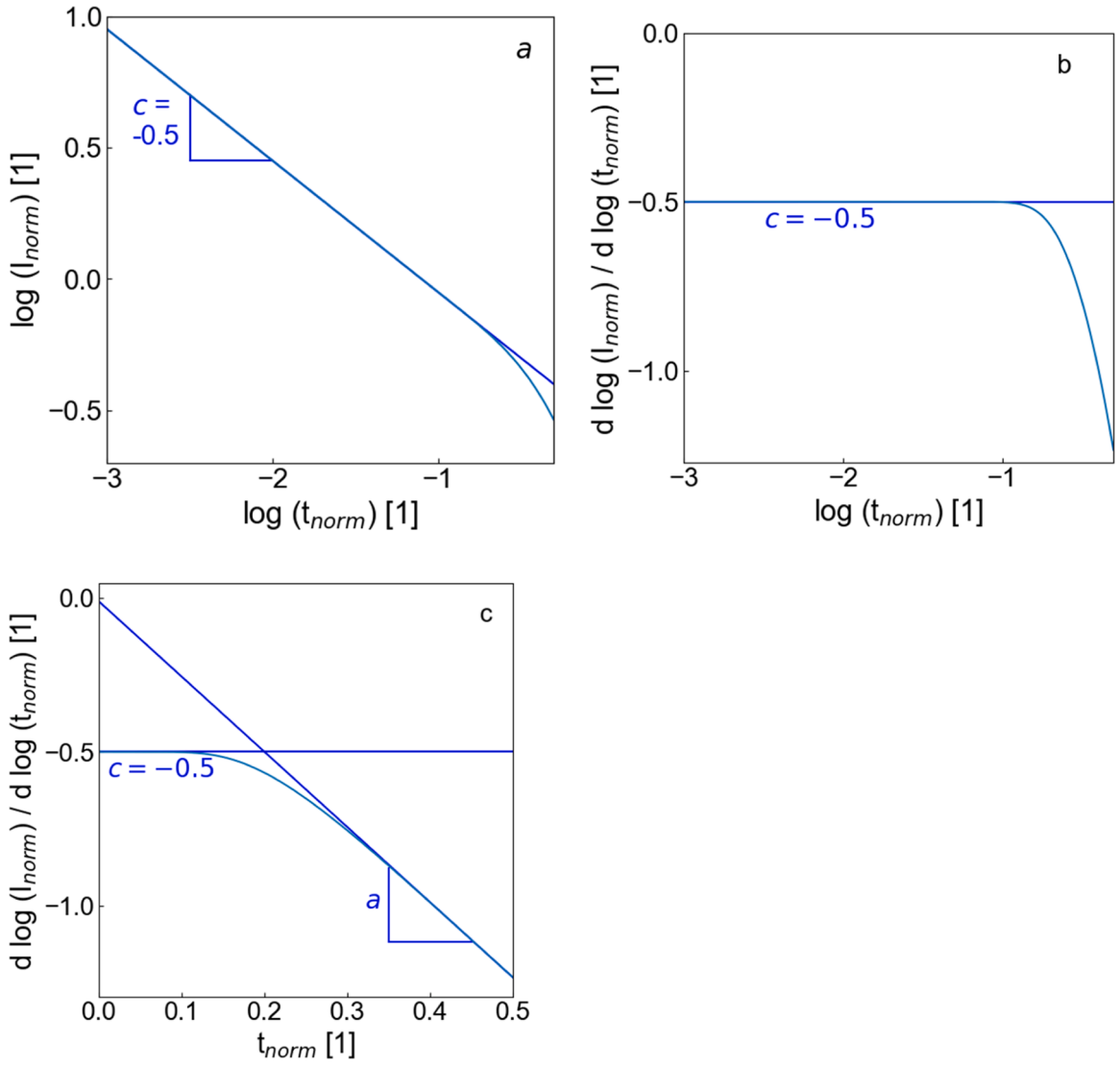

Fig. 4. Normalized representations of the current transient due to a potential step calculated according to Equ. (2). (a) In the double-logarithmic plot the current shows a linear behaviour with a slope of $c = -0.5$ for small times. (b) Derivative of the current transient in the double-logarithmic plot in dependence of the time in logarithmic representation. At small times the value of the derivative is $c = -0.5$. (c) Derivative of the current transient in the double-logarithmic plot in dependence of the time in linear representation. The period of the constant value $c = -0.5$ is followed by a period with a constant slope a.

from the influence of electron transfer kinetics [7]. Montella's paper shows the appearance of current transients under mixed control.

In this paper, the applicability of the potential step chronoamperometry using the long-time approximation to determine the diffusion coefficient D is further investigated. As an example, the method is used to determine the diffusion coefficient of H in Pd. Samples with thicknesses in different orders of magnitude are compared. To determine the diffusion controlled regime in the measured data, the result is compared to numerical calculations assuming a diffusion-controlled process. A literature review extends the findings for H in Pd to the more general case.

2. Experimental

Potential step chronoamerometry is performed on Pd sheets of 25, 55 and 250 μm thickness and on Pd thin films of 100 nm thickness. The Pd sheets were purchased from HMW Hauner GmbH& Co. KG with a purity of at least 99.5 %. The thin films are prepared on Al_2O_3 (0001) substrates purchased from CrysTec by ion beam sputtering in a UHV system with a background pressure of about 10^{-8} mbar with Pd targets with a purity of at least 99.9 %. All experiments are performed at room temperature. The loading cell geometry allows contact between the sample and the electrolyte on one side of the sample only, so that the setup is suitable for bulk samples as well as thin film samples on substrates. The sample is loaded and unloaded with hydrogen in a three electrodes setup with the sample as the working electrode and a platinum or palladium hydride counter electrode (Fig. 5). The potentials are measured against a Hg/HgO reference electrode. As electrolyte for the hydrogen loading and unloading of palladium, 6 M KOH is used. As described in [12], the electrolyte is bubbled with argon gas for 30 min to reduce its O_2 content. A VMP-3 (Bio-Logic SAS) potentiostat is used for the measurements of the 25 and 55 μm thick samples, and for these samples only, the electrolyte was not bubbled. A LPG 03 (Bank Elektronik) potentiostat is used for the samples of 250 μm thickness and the thin films. The measurement results are not expected to depend on the potentiostat.

Table 1 summarizes the parameters of the exemplary measurements shown in Figs. 6–8. The H concentrations (initial and final) are given in number of H-atoms per number of Pd atoms, H/Pd. They result from integrating the current over time and using Faraday's law. The other measurements shown in Fig. 10 possess an initial hydrogen

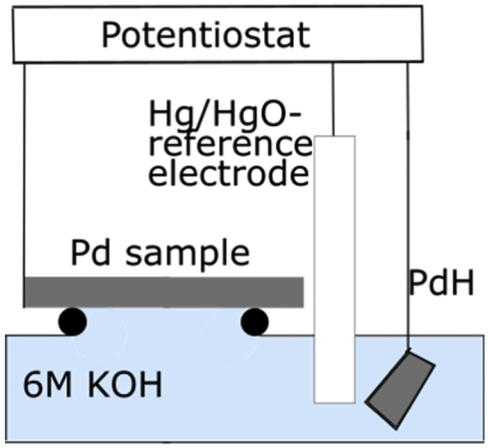

Fig. 5. Three electrodes setup with the Pd sample as working electrode, the Hg/HgO reference electrode, a PdH counter electrode and the 6 M KOH electrolyte. The sample is placed on a rubber ring of 9 mm diameter (black circle). The part of the sample that is in contact with the electrolyte is its electrode area used to calculate the current densities.

Table 1
Parameters of the exemplary measurements shown in Fig. 6, Fig. 7 and Fig. 8.

Sample thickness [µm]	Loading potential [mV vs. Hg/HgO]	Unloading potential [mV vs. Hg/HgO]	Initial H concentration [H/Pd]	Final H concentration [H/Pd]
0.1	−1050	−200	0.27	0.15
55	−1100	−200	0.003	0.02
250	−1050	−200	0.014	0.005

concentration of 0.003 to 0.02 H/Pd. They are measured with a potential step from −1050 or −1100 mV to −200 mV vs. Hg/HgO. Due to the large potential steps and the corresponding large concentration steps the diffusion coefficient might not be constant throughout the experiment.

3. Results

In the following, some aspects and discrepancies regarding the determination of the diffusion coefficient will be addressed, originating from the method and the data representation.

Fig. 6(a) shows an exemplary measurement for the unloading of a 55 µm thick Pd sheet. To determine the diffusion coefficient D according to Equ. (6), the semi-logarithmic plot of the current transient as a function of time in Fig. 6(b) is used. If the slope m is determined in the period marked in red in b), the resulting apparent diffusion coefficient is $D^{Pd}_{H,app} = 2.5{\cdot}10^{-8}$ cm^2/s. This is more than one order of magnitude lower than the literature value of $D^{Pd}_{H} = 3.3{\cdot}10^{-7}$ cm^2/s [13]. The measurement results are more clearly depicted by plotting the derivative of the double-logarithmic dependency versus time (Fig. 6(c)). From this plot the slope a is determined and inserted into Equ. (8) yielding $D^{Pd}_{H,app} = 2.1{\cdot}10^{-7}$ cm^2/s, in better agreement with the literature value.

By using the latter value of the diffusion coefficient, Equ. (2) can be fitted to the measured current transient. This calculated current transient then shows the current transient of an idealy diffusion controlled process. Hence, by fitting Equ. (2) to the measured data the diffusion-controlled regime can be identified. In the first 20 s of the unloading process, both the measured and the fitted transient show the constant value of $c = -0.5$. This value is associated with semi-infinite diffusion. In total, measurement and calculation are in good agreement within about the first 70 s. In this period, the slope m marked in yellow in Fig. 6(b) is determined and inserted in Equ. (6) yielding $D^{Pd}_{H,app} = 2.5{\cdot}10^{-7}$ cm^2/s. This value is in good agreement with literature, too (see Table 2).

At longer times, however, the measurement and the calculated transient for a diffusion-controlled process according to Equ. (2) deviate strongly. In summary, the measurement can be divided into 3 successive periods:

(1) Semi-infinite diffusion: In the semi-logarithmic representation the slope of the current transient declines. In the d log(j) / d log(t) vs. t plot it gives a constant value of −0.5.
(2) Diffusion-controlled regime: Measurement and fit of the declining transients are in good agreement according to Equ. (2).
(3) At longer times: The measurement deviates strongly from the calculated diffusion-controlled current transient.

Similar findings are shown in Ref. [14] (Fig. 5) for Li insertion in $LiMn_2O_4$ and in Ref. [15] (Fig. 7) for Li insertion in $LaNi_{3.55}Mn_{0.4}Al_{0.3}Co_{0.4}Fe_{0.35}$. Also, Ref. [16] (Fig. 3b) reported such a behaviour for Li-ions in Nb_2O_5 nanoparticles for a slightly different method applying multiple, smaller potential steps.

Fig. 7(a) shows the potential step chronoamperometry of a 100 nm thick Pd thin film, Fig. 7(b) gives its values in semi-logarithmic representation. Fig. 7(c) presents the calculation according to Equ. (2) only. The diffusion coefficient used for the calculation is $D^{Pd}_{H} = 2.1{\cdot}10^{-7}$ cm^2/s, being the same as in Fig. 6(c) for comparison. According to this, the period of semi-infinite diffusion spans only a fraction of a millisecond. The value then drops below d log (j) / d log (t) = −10 within the first millisecond. The measurement (not shown here) reveals values between d log (j) / d log (t) = −2 and d log (j) / d log (t) = 0 for the first 200 s. In the semi-logarithmic representation of Fig. 7(b) the current transient becomes a linear equation at long times. Hence, the period marked in red seems suitable for determining the diffusion coefficient according to Equ. (6) giving a value of $D^{Pd}_{H,app} = 1.7{\cdot}10^{-13}$ cm^2/s. This differs by about 6 orders of magnitude from the literature value for bulk Pd. The hydrogen concentration of the sample is in the two-phase region of solid solution and hydrite phase (Table 1). However, the current transient does not show characteristic two-phase behaviour as described in [10].

Fig. 8(a) shows an exemplary potential step chronoamperometry measurement for a 250 µm thick sample, given in Fig. 8(b) in semi-logarithmic representation of the current transient. The period that is conventionally used to determine the diffusion coefficient according to Equ. (6) is marked in yellow in b). Fig. 8(c) shows the derivative in the double logarithmic plot against the linear time. In the calculation, the diffusion coefficient $D^{Pd}_{H} = 3.1{\cdot}10^{-7}$ cm^2/s is fitted to the measured curve. Here, the measurement is in good agreement with the calculation throughout the experiment, with the exception of short times. The period that is used to determine the diffusion coefficient according to Equ. (8) is marked in yellow in (c). The resulting apparent diffusion coefficient $D^{Pd}_{H,app} = 3.1{\cdot}10^{-7}$ cm^2/s is in good agreement with the literature value (see Table 2).

Potential step chronoamperometry of 250 µm thick samples is conducted with different unloading potentials from −400 to 0 mV. Within this potential range, the current transient is unaffected by the potential. Additionaly, the hydrogen concentration in the sample is increased by setting a lower loading potential or longer loading times within the solid solution regime. Even when the resulting unloading current changes by more than one order of magnitude, the slope in the semilogarithmic plot remains within the order of magnitude. Accordingly, the influence of potential and concentration on the apparent diffusion coefficient is small in comparison to the influence of sample thickness.

Fig. 9 summarizes the calculation of the derivatives of the current transients in the double logarithmic plot resulting for different sample thicknesses according to Equ. (2). Apparently, the period of constant value $c = -0.5$ that is associated with semi-infinite diffusion has a longer duration for a thicker sample. Also, the slope a in the subsequent, still diffusion-controlled period is less steep for a thicker sample. As described in Figs. 6 and 7, the measured data is in good agreement with the fitted curve only for the duration of the semi-infite diffusion, and a

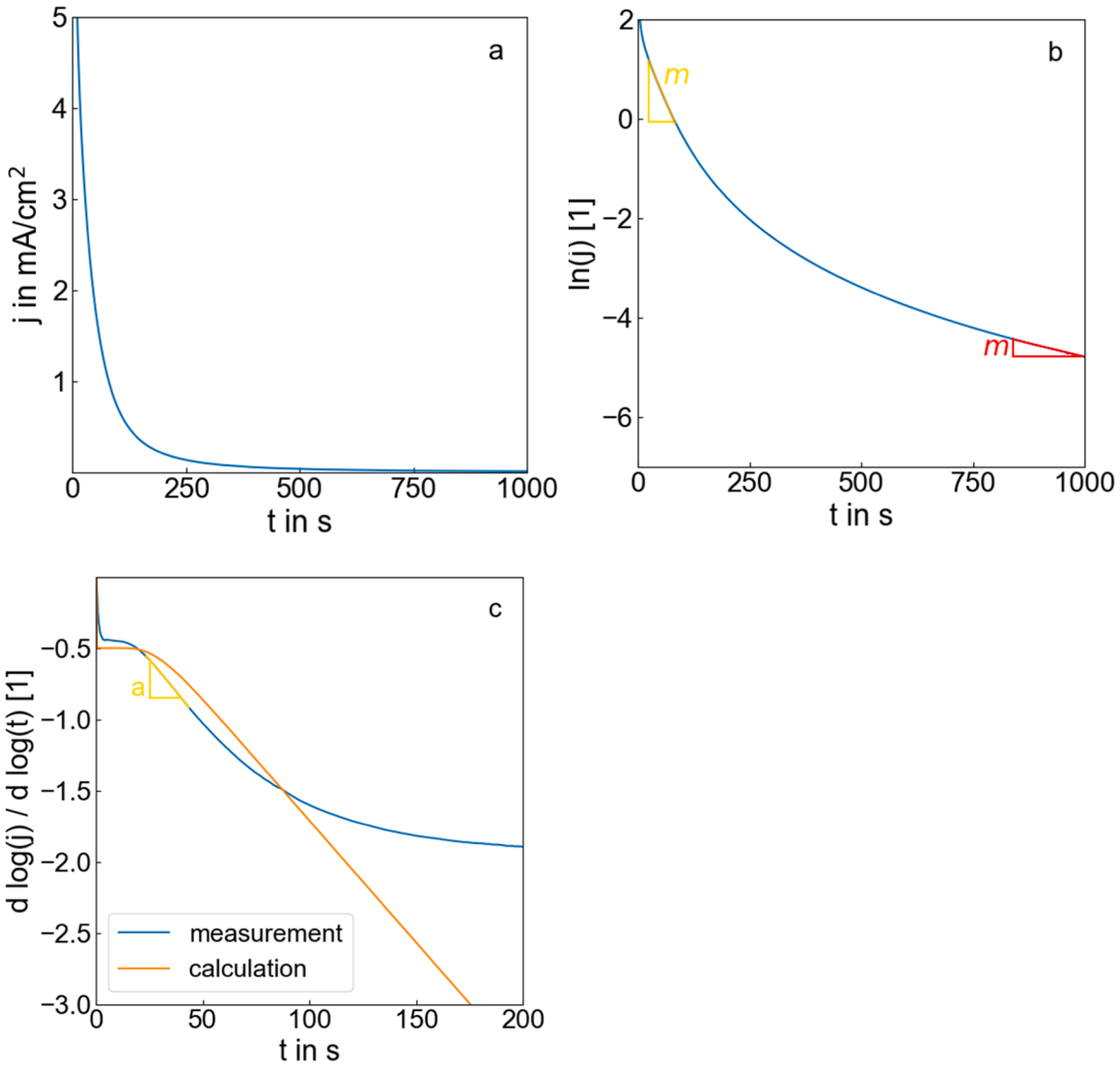

Fig. 6. Potentiostatic unloading of a 55 µm thick Pd sheet. (a) Linear representation of the current transient. (b) Semi-logarithmic representation of the current transient. The slopes m in the yellow and red period are used to determine the diffusion coefficient D_H^{Pd} according to Equ. (6). The results are shown in Table 2. (c) Derivative of the double-logarithmic representation as a function of time, analogue to Fig. 4(c). Fit of Equ. (2) to the measured data, to determine the diffusion controlled regime. The experimental curve is smoothed for better readability. The fit according to Equ. (2) yields an apparent diffusion coefficient of $D_{H,app}^{Pd} = 2.1 \cdot 10^{-7}$ cm^2/s. The slope a of the measured data in the yellow period is used to determine the diffusion coefficient D_H^{Pd} according to Equ. (8). The result is shown in Table 2.

subsequent period. For longer times, the measured data is not in good agreement with the fitted curve.

4. Discussion

In the following, the discrepancies between the measured data and the fitted curves for hydrogen in Pd are further discussed. The restrictions of the applicability of the potential step chronoamperometry using long-time approximation are then identified in a more general case.

The fitted current transients shown in Fig. 6(c), Fig. 7(c) and Fig. 8(c) are calculated according to Equ. (2). As this equation is derived directly from the diffusion equations, they represent current transients of ideal diffusion controlled hydrogen unloading processes. Montella [8] calculated current transients associated with intercalation processes that are under mixed control of diffusion, of charge transfer or of ohmic drop influence. The slight deviations between calculation and measurement at the beginning of the measurement in the period of semi-infinite diffusion can be satisfactorily explained with regard to Montella's calculations.

As described above, the measured current transient of the 55 µm thick Pd sample is in good agreement with the calculation of the current transient for a diffusion-controlled process within the first about 70 s. Therefore, the hydrogen unloading process can be regarded as being diffusion-controlled within this period of time. At longer times than 70 s, the measured curve deviates strongly from the calculation. For this sequence, the process is not diffusion-controlled any more. It is assumed that it is controlled by another step in the process, for example by charge transfer at the sample surface. This behaviour is even more pronounced for the current transient of the 100 nm thin film sample. Its kinetics are not diffusion-controlled at any period of the measurement. Throughout the entire measurement period, it appears that surface processes control the unloading process. Conversely, the current transient of the 250 µm thick bulk sample is diffusion-controlled throughout the entire measurement. This interpretation of the current transient is in accordance with Ref. [16] for Li-ions in Nb_2O_5. Here, the author used two separate exponential functions both being diffusion and charge transfer controlled as calculated by Montella [8] to model the current transient.

Our data reveal the necessessity of a diffusion-controlled process for the determination of a reliable diffusion coefficient. This aspect was also

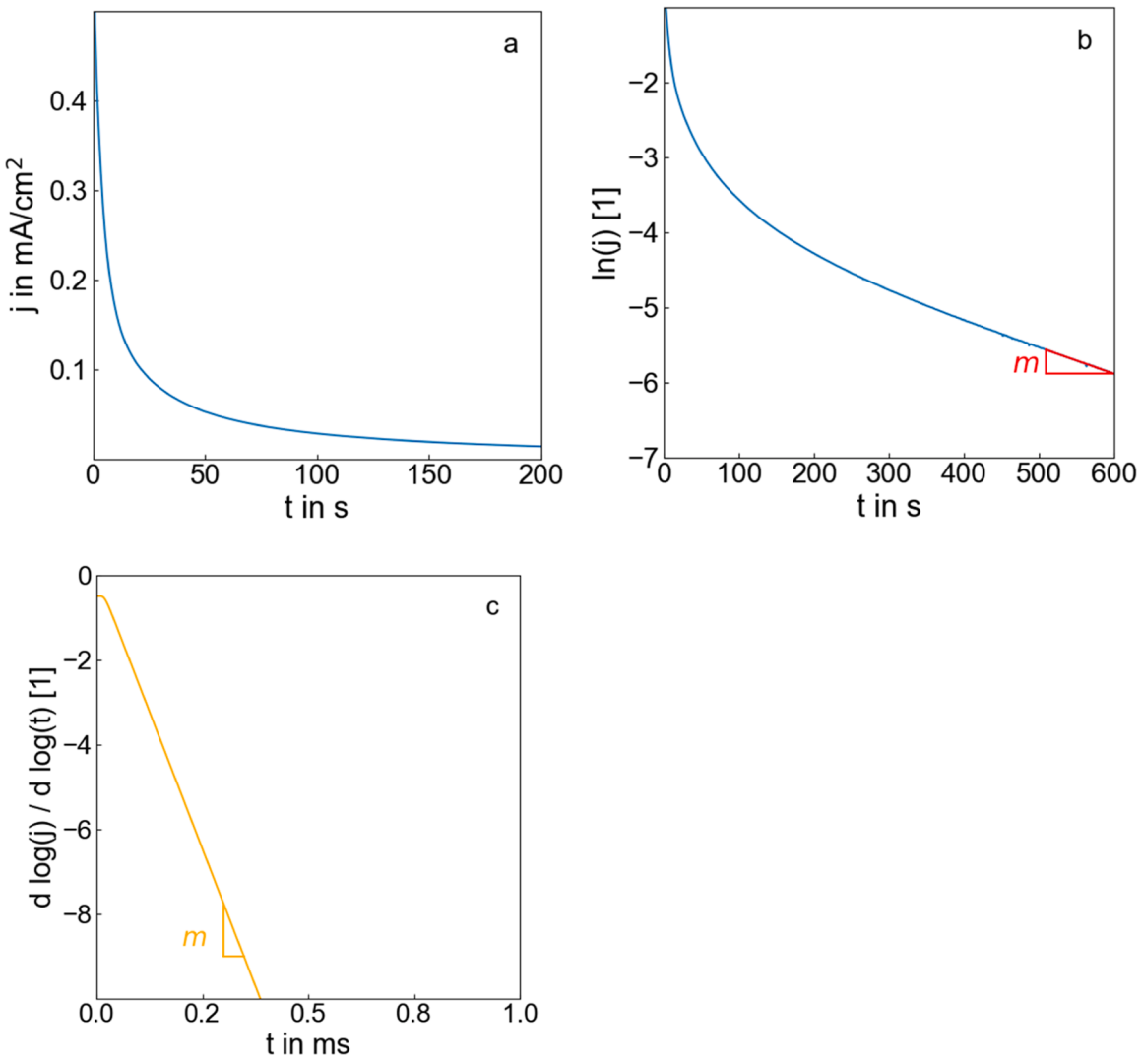

Fig. 7. Potentiostatic unloading of a 100 nm thick Pd thin film. (a) Linear representation of the current transient. (b) Semi-logarithmic representation of the current transient. The slope m in the red period is used to determine the diffusion coefficient D_H^{Pd} according to Equ. (6). The result is shown in Table 2. (c) Calculation of the derivative of the double logarithmic representation as a function of time, analogue to Fig. 4(c), according to Equ. (2). A diffusion coefficient of $D_H^{Pd} = 2.1 \cdot 10^{-7}$ cm²/s is assumed for the calculation.

emphasized by Lee and Pyun [10]. This implies that the determination of diffusion coefficients using the slope *m* marked in red in Fig. 6(b) and Fig. 7(b) nessecarily leads to incorrect diffusion coefficients.

Interestingly, the value of the slope *m* that is used to determine the diffusion coefficient according to Equ. (6) for long times (marked in red in Fig. 6(b) and Fig. 7(b)) gives almost the same value regardless of the sample thickness. On the contrary, the slope measured specifically in the diffusion-controlled period has a significantly different value of *m*, see Fig. 6. To explore this effect in depth, logarithmising Equ. (6) gives the following equation:

$$log(D) = log\left(\frac{4}{\pi^2}|m|\right) + 2 \cdot log(L) \tag{9}$$

If *m* is constant, this equation becomes a linear equation with constant offset and a slope of $s = 2$ cm/s, in double logarithmic representation of the apparent diffusion coefficient *D* on the diffusion length *L*. This implicit behaviour is confirmed empirically when a variety of literature values is revisited: Fig. 10 shows the calculated diffusion coefficients published in different papers [1],[2],[9],[14–28] together with the results from Table 2: In these papers, diffusion coefficients of Li-ions as well as H in different host materials are reported. The sample geometries were either spheres or sheets that were in contact with either one or both sides with the electrolyte. Several different electrolytes were used. Where several measurement points from a single paper are shown, Table 3 briefly names the parameters under investigation. Where the diffusion coefficients at room temperature are not given, we calculated the corresponding values for room temperature. Fig. 10 also shows a linear regression of all measurement points. The points are weighted so that each source has the same weight. The slope of this balance line is 1.5 cm/s. This is slightly different from the calculated value of 2 cm/s, that is also marked in Fig. 8 with a dotted line. This means that the slope *m* in the time-sequences chosen in the literature was not perfectly constant, but it was close to being a constant. Ref [16] is not on this balace line, as during the calculation the different regimes were taken into account. Hence, distinguishing between the different regimes is essential for correct interpretation of the current transients, as it leads to significantly different results.

The slope *m* is the output of the potential step chronoamperometry measurement. However, apparently for a variety of different measurements for different intercalating systems it is almost a constant, independent of the experimental details (see Fig. 8). This unexpected correlation reveals directly, that the determined diffusion coefficients given in these publications might be not correct, because they were possibly determined without taking the diffusion regimes into account.

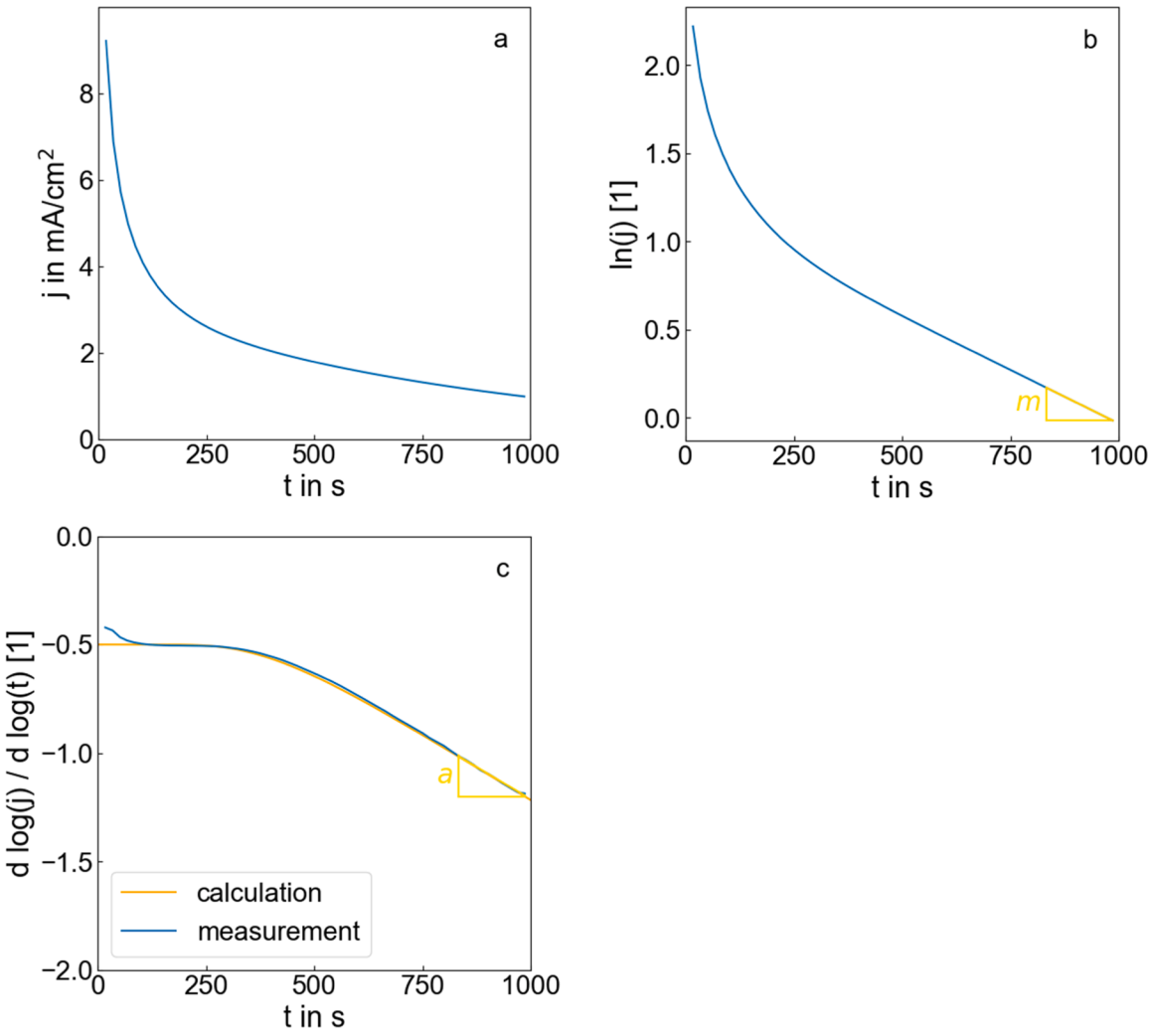

Fig. 8. Potentiostatic unloading of a 250 µm thick Pd sample. (a) Linear representation of the current transient. (b) Semi-logarithmic representation of the current transient. The slope m in the yellow period is used to determine the diffusion coefficient D_H^{Pd} according to Equ. (6). The result is shown in Table 2. (c) Derivative of the double-logarithmic representation as a function of time, analogue to Fig. 4(c). For the calculation a diffusion coefficient of $D_H^{Pd} = 3.1 \cdot 10^{-7}$ cm²/s is assumed. The slope a in the yellow period is used to determine the diffusion coefficient D_H^{Pd} according to Equ. (8). The result is shown in Table 2.

Table 2
Determination of the apparent diffusion coefficient $D_{H,app}^{Pd}$ according to Equs. (6) and (7) as from Fig. 6, Figs. 7 and 8. The apparent diffusion coefficient shows a dependence on the sample thickness. This apparent effect is critically discussed in the discussion section.

Sample thickness L [µm]	Slope m in ln(j) vs. t-plot [1/s] to insert into Equ. (6)	Slope a in d log(j)/d log (t) vs. t plot [1/s] to insert into Equ. (8)	$D_{H,app}^{Pd}$ [cm²/s]
250	$-0.0012 \pm 8 \cdot 10^{-5}$		$3.2 \cdot 10^{-7} \pm 2 \cdot 10^{-8}$
250		$-0.0012 \pm 3 \cdot 10^{-5}$	$3.1 \cdot 10^{-7} \pm 6 \cdot 10^{-9}$
55	-0.002 ± 0.0001		$2.5 \cdot 10^{-8} \pm 1 \cdot 10^{-9}$
55	-0.021 ± 0.013		$2.5 \cdot 10^{-7} \pm 1 \cdot 10^{-8}$
55		-0.019 ± 0.002	$2.1 \cdot 10^{-7} \pm 3 \cdot 10^{-8}$
0.1	-0.004 ± 0.0008		$1.7 \cdot 10^{-13} \pm 3 \cdot 10^{-14}$

As shown above, the given values are only correct if the slope is determined in the diffusion-controlled period of the measurements.

The present paper demonstrates that the unloading process is not

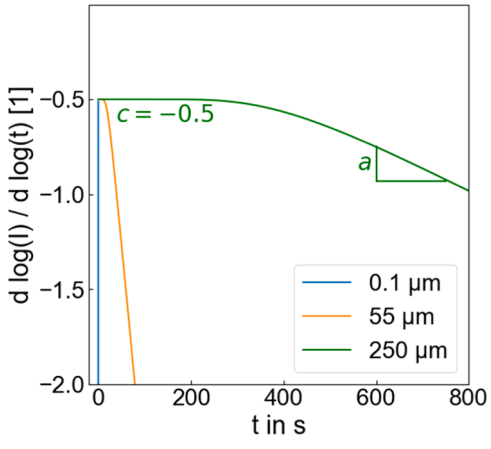

Fig. 9. Summary of the fits of the current transients in the double-logarithmic plot against the linear time according to Equ. (2) for the different investigated sample thicknesses. The same diffusion coefficient of $D_H^{Pd} = 3.1 \cdot 10^{-7}$ cm²/s is used for the calculation of the three current transients. The durations of constant transient and the slopes in the subsequent period vary strongly for the different sample thicknesses.

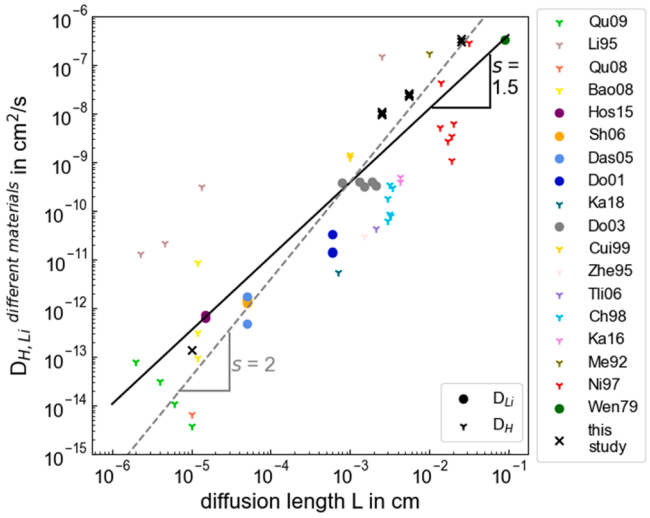

Fig. 10. Literature review of the potential step chronoamperometry using the long-time approximation. The references as well as an overview of their experimental setups are listed in Table 3. The straight line is a linear regression of all the measurement points. The dotted line is a line with slope $s = 2$. All hydrogen diffusion coefficients are marked with a cross, all lithium diffusion coefficients are marked with a circle.

necessarily diffusion controlled but different regimes can occur, even if always the same materials system of Pd-H is studied. For very thin films, for example, surface processes seem to dominate the kinetics of the hydrogen unloading process. If this is not taken into account, the evaluations will lead to incorrect results. It is therefore necessary to ensure that the potential step chronoamperometry in the long-time approximation is performed in the diffusion-controlled period.

The diffusion-controlled period in the experiment can be determined by the following way. For a single film without phase transformation the current transient of an ideally diffusion controlled process in a d log (I) / d log (t) vs. t plot has the characteristic shape shown in Fig. 4(c): At short times, it has a constant value of $c = -0.5$ and at long times, it has a constant slope a. If it is possible to choose the diffusion lenght L so that the current transient calculated according to Equ. (2) can be fitted to this characteristic shape, a diffusion controlled process can be assumed. Lee and Pyun [10] present more sophisticated models for the current transient, for example including a phase transition. Conceivably, fitting a current transient to a more sophisticated model also proves diffusion control.

For a better overview the slopes in the different contexts are summarized in Table 4.

5. Conclusion

Determination of the diffusion coefficient of intercalating species by potential step chronoamperometry using long-time approximation requires explicit consideration of the diffusion regime. This is demonstrated on the example of Pd-H samples of different thicknesses and by a critical literature review. It is suggested that the unloading process is not necessarily simply controlled by the interstitial diffusion in the host material, but other rate-limiting steps can arise. Consequently, for a reliable determination of the diffusion coefficient the diffusion-controlled regime must be specified beforehand. This can be done by fitting the measured transient with a diffusion-controlled transient, according to Equ. (2). Therefore, the sample thickness must be chosen so that the characteristic shape of the current transient for the diffusion in a plane sheet is recognizable. If the diffusion-controlled regime can be specified, the determination of the diffusion coefficient by chronoamperometry is reliable. If it is not possible to differentiate between diffusion-controlled and non-diffusion-controlled period, other techniques such as permeation measurements need to be applied to determine a reliable diffusion coefficient [30]. We suggest that literature diffusion data measured by potential step chronoamperometry needs to be critically revisited.

Table 3
References and their experimental setups used in Fig. 10.

Author (+et.al.), Year, citation	Diffusing Species in host material	Process and sample geometry	Electrolyte	Variable
Qu09, [19]	H in MgH_2	Unloading one side of the sample	6 M KOH	Sample thickness
Li95, [18]	H in Pd	Unloading one side of the sample	6 M KOH	Sample thickness
Qu08, [17]	H in Mg	Unloading one side of the sample	6 M KOH	-
Bao08, [20]	H in $Mg_{2,4,6}Ni$	Unloading one side of the sample	1 M KOH	Composition of the host material
Hos15, [1]	Li in $LiMn_{1-x}Fe_xPO_4$	Unloading of powder	ethylene carbonate and diethyl carbonate 1:2 containing 1 M $LiPF_6$	Composition of the host material from $x = 0.75$ to $x = 1$
Sh06, [14]	Li-ions in $LiMn_2O_4$	Loading one side of the sample	ethylene carbonate and diethyl carbonate 1:1 containing 1 M LiPF6	Calcination temperature
Das05, [21]	Li-ions in $Li_{1.40}Mn_2O_4$	Loading one side of the sample	ethylene carbonate and diethyl carbonate 1:2 containing 1 M LiPF6	Cycling
Do01, [22]	Li-ions in $LiMn_2O_4$	Loading of a particle	1 M $LiClO_4$ /propylene carbonate and ethylene carbonate 1:1	Applied potentials
Ka18, [2]	H in $LaGaO_3$	Discharging of particles	7 M KOH	-
Do03, [23]	Li-ions in $LiMn_2O_4$	Loading of particles	1 M $LiClO_4$ /propylene carbonate and ethylene carbonate 1:1	Particle Diameter
Cui99, [24]	H in $Mg_{1.9}V_{0.1}Ni_{0.8}Al_{0.2}$	Unloading of particles	6 M KOH	Density of discharge
Zhe95, [9]	H in $LaNi_{4.25}Al_{0.75}$	Loading of particles	6 M KOH	-
Tli06, [15]	H in $LaNi_{3.55}Mn_{0.4}Al_{0.3}Co_{0.4}Fe_{0.35}$	Unloading of particles	7 M KOH	-
Ch98, [25]	H in Ni- and Zr-based alloys	Unloading of particles	6 M KOH	Composition of the host material
Ka16, [26]	H in $LaGaO_3$	Discharging of particles	7 M KOH	State of charge
Me92, [27]	H in Pd	Unloading from both sides	0.1 M LiOH	-
Ni97, [28]	H in Pd and Ni-based alloys	Unloading of particles	1 M KOH	Host material
Wen79, [29]	Li in LiAl	Unloading of the sample	Molten LiCl-KCl	-
This study	H in Pd	Unloading of one side	6 M KOH	thickness

Table 4
Overview of the slopes used in the different contexts.

Name of the slope	Meaning and related equations
m	Slope in the ln(I) vs. t plot of Equ. (2) for long times. Used to determine the diffusion coefficient with Equ. (6). $D = \frac{4}{\pi^2}\left\|m\right\|L^2$ (6)
c	Slope in the double-logarithmic log(I) vs. log(t) plot of Equ. (2) for short times. The slope $c = 0.5$ becomes the constant value $c = 0.5$ if the derivative is plotted. $I(t) = \frac{2FA(c_s - c_0)D}{L}\sum_{n=0}^{\infty} exp\left(-\frac{D(2n+1)^2\pi^2}{4L^2}\cdot t\right)$ (2)
a	Slope in the derivative of the double-logarithmic log(I) vs. log(t) plot vs. linear time at long times. Used to determine the diffusion coefficient with Equ. (8). $D = \frac{4}{\pi^2}\left\|a\right\|L^2$ (8)
s	Slope in the double-logarithmic representation of Equ. (6) in a plot of D vs. L $log(D) = log\left(\frac{4}{\pi^2}\|m\|\right) + \underbrace{2}_{s}\cdot log(L)$ (9)

CRediT authorship contribution statement

Magdalena Seiler: Writing – original draft, Visualization, Investigation, Formal analysis. **Giorgia Guardi:** Supervision. **Stefan Wagner:** Writing – review & editing, Supervision. **Astrid Pundt:** Writing – review & editing, Supervision.

Declaration of competing interest

The authors declare that they have no known competing financial interests or personal relationships that could have appeared to influence the work reported in this paper.

Acknowledgements

We acknowledge Dennis Triller (KIT, IAM-ESS) for his support with Potentiostat measurements.

Data availability

Data from "Applicability range of Potential Step Chronoamperometry for the Determination of the Diffusion Coefficients of Hydrogen and Lithium in Host Materials" (Original data) (Zenodo)

References

[1] K. Hoshina, T. Sasakawa, N. Takami, H. Munakata, K. Kanamura, Lithium diffusion in cation-mixing-free LiMn1-xFexPO4 synthesized by hydrothermal process, J. Electrochem. Soc. 162 (2015) A2827.
[2] A. Kaabi, M. Tliha, A. Dhahri, C. Khaldi, N. Fenineche, O. Elkedim, J. Lamlouli, Effect of temperature on behavior of perovskite-type oxide LaGaO3 used as a novel anode material for Ni-MH secondary batteries, Int. J. Energy Res. 42 (2018) 2953–2960.
[3] S. Lynch, Hydrogen embrittlement phenomena and mechanisms, Corros. Rev. 30 (2012) 105–123, https://doi.org/10.1515/corrrev-2012-0502.
[4] T. Erika, F. Ricardo, R. Fabricio, Z. Fernando, D. Verónica, Electrochemical and metallurgical characterization of ZrCr1-xNiMox AB2 metal hydride alloys, J. Alloys Compd. 649 (2015) 267–274.
[5] J. Crank, The Mathematics of Diffusion, Oxford Univertity Press, 1975.
[6] jost, Diffusion in solids, Liquids and Gases, Academic press inc., Publishers New York, 1955.
[7] P. Zanello, C. Nervi, F.F. De Biani, Inorganic electrochemistry: theory, Practice and Application, Royal Society of Chemistry, 2019.
[8] C. Montella, Discussion of the potential step method for the determination of the diffusion coefficients of guest species in host materials: part I. Influence of charge transfer kinetics and ohmic potential drop, J. Electroanal. Chem. 518 (2002) 61–83.
[9] G. Zheng, B.N. Popov, R.E. White, Electrochemical determination of the diffusion coefficient of hydrogen through an LaNi4. 25Al0. 75 electrode in alkaline aqueous solution, J. Electrochem. Soc. 142 (1995) 2695.
[10] J.-W. Lee, S.-I. Pyun, Anomalous behaviour of hydrogen extraction from hydride-forming metals and alloys under impermeable boundary conditions, Electrochim. Acta 50 (2005) 1777–1805.
[11] H.-C. Shin, S.-I. Pyun, An investigation of the electrochemical intercalation of lithium into a Li1- δCoO2 electrode based upon numerical analysis of potentiostatic current transients, Electrochim. Acta 44 (1999) 2235–2244.
[12] G. Guardi, A. Sarapulova, S. Dsoke, S. Wagner, L. Pasquini, A. Pundt, Controlled hydrogen loading of magnesium thin films in KOH—Effects on the hydride nucleation and growth regimes. Micro, MDPI, 2024, pp. 765–777.
[13] R. Kirchheim, A. Szökefalvi-Nagy, U. Stolz, A. Speitling, Hydrogen in deformed and amorphous Pd80Si20 compared to hydrogen in deformed and crystalline palladium, Scr. Metall. 19 (1985) 843–846.
[14] F.-Y. Shih, K.-Z. Fung, Effect of annealing temperature on electrochemical performance of thin-film LiMn2O4 cathode, J. Power Sources 159 (2006) 179–185.
[15] M. Tliha, H. Mathlouthi, C. Khaldi, J. Lamloumi, A. Percheron-Guégan, Electrochemical properties of the LaNi3. 55Mn0. 4Al0. 3Co0. 4Fe0. 35 hydrogen storage alloy, J. Power Sources 160 (2006) 1391–1394.
[16] Y. Zhou, M. Frajnkovič, A. Likitchatchawankun, O. Munteshari, B.-A. Mei, L. Pilon, Three-dimensional step potential electrochemical spectroscopy (SPECS) simulations of porous pseudocapacitive electrodes, Electrochim. Acta 505 (2024) 144934.
[17] J. Qu, Y. Wang, L. Xie, J. Zheng, Y. Liu, X. Li, Superior hydrogen absorption and desorption behavior of Mg thin films, J. Power Sources 186 (2009) 515–520.
[18] Y. Li, Y.-T. Cheng, Hydrogen diffusion and solubility in palladium thin films, Int. J. Hydrog. Energy 21 (1996) 281–291.
[19] J. Qu, B. Sun, R. Yang, W. Zhao, Y. Wang, X. Li, Hydrogen absorption kinetics of Mg thin films under mild conditions, Scr. Mater. 62 (2010) 317–320.
[20] S. Bao, Y. Yamada, M. Okada, K. Yoshimura, Electrochromic properties of Pd-capped Mg–Ni switchable mirror thin films, Electrochemistry 76 (2008) 282–287.
[21] S. Das, S. Majumder, R. Katiyar, Kinetic analysis of the Li+ ion intercalation behavior of solution derived nano-crystalline lithium manganate thin films, J. Power Sources 139 (2005) 261–268.
[22] K. Dokko, M. Nishizawa, M. Mohamedi, M. Umeda, I. Uchida, J. Akimoto, Y. Takahashi, Y. Gotoh, S. Mizuta, Electrochemical studies of Li-ion extraction and insertion of LiMn2 O 4 single crystal, Electrochem. Solid-State Lett. 4 (2001) A151.
[23] K. Dokko, M. Mohamedi, M. Umeda, I. Uchida, Kinetic study of Li-ion extraction and insertion at LiMn2 O 4 single particle electrodes using potential step and impedance methods, J. Electrochem. Soc. 150 (2003) A425.
[24] N. Cui, J. Luo, Electrochemical study of hydrogen diffusion behavior in Mg2Ni-type hydrogen storage alloy electrodes, Int. J. Hydrog. Energy 24 (1999) 37–42.
[25] J. Chen, S. Dou, D. Bradhurst, H. Liu, Studies on the diffusion coefficient of hydrogen through metal hydride electrodes, Int. J. Hydrog. Energy 23 (1998) 177–182.
[26] A. Kaabi, M. Tliha, A. Dhahri, C. Khaldi, J. Lamloumi, Study of electrochemical performances of perovskite-type oxide LaGaO3 for application as a novel anode material for Ni-MH secondary batteries, Ceram. Int. 42 (2016) 11682–11686.
[27] G. Mengoli, M. Fabrizio, C. Manduchi, G. Zannoni, Surface and bulk effects in the extraction of hydrogen from highly loaded Pd sheet electrodes, J. Electroanal. Chem. 350 (1993) 57–72.
[28] T. Nishina, H. Ura, I. Uchida, Determination of chemical diffusion coefficients in metal hydride particles with a microelectrode technique, J. Electrochem. Soc. 144 (1997) 1273.
[29] C.J. Wen, B. Boukamp, R.A. Huggins, Wjj. Weppner, Thermodynamic and mass transport properties of LiAl, J. Electrochem. Soc. 126 (1979) 2258.
[30] N. Boes, H. Züchner, Electrochemical methods for studying diffusion, permeation and solubility of hydrogen in metals, J. Common Met. 49 (1976) 223–240, https://doi.org/10.1016/0022-5088(76)90037-0.